ACS Pharmacology & Translational Science

pubs.acs.org/ptsci

Article

Modulation of Amyloid and Tau Aggregation to Alleviate Cognitive Impairment in a Transgenic Mouse Model of Alzheimer's Disease

Sohui Park,○ Jisu Shin,○ Kyeonghwan Kim,○ Darong Kim,○ Won Seok Lee, Jusuk Lee, Illhwan Cho, In Wook Park, Soljee Yoon, Songmin Lee, Hye Yun Kim,* Ji Hoon Lee,* Ki Bum Hong,* and YoungSoo Kim*

Cite This: *ACS Pharmacol. Transl. Sci.* 2024, 7, 2650−2661

Read Online

ACCESS | Metrics & More | Article Recommendations | Supporting Information

ABSTRACT: Aggregation of misfolded amyloid-β (Aβ) and hyperphosphorylated tau proteins to plaques and tangles, respectively, is the major drug target of Alzheimer's disease (AD), as the former is an onset biomarker and the latter is associated with neurodegeneration. Thus, we report a small molecule drug candidate, DN5355, with a dual-targeting function toward aggregates of both Aβ and tau. DN5355 was selected through a series of four screenings assessing 52 chemicals for their functions to inhibit and reverse the aggregation of Aβ and tau by utilizing thioflavin T. When orally administered to AD transgenic mouse model 5XFAD, DN5355 significantly reduced cerebral Aβ plaques and hyperphosphorylated tau tangles. In Y-maze spontaneous alteration and contextual fear conditioning tests, 5XFAD mice showed amelioration of cognitive deficits upon the oral administration of DN5355.

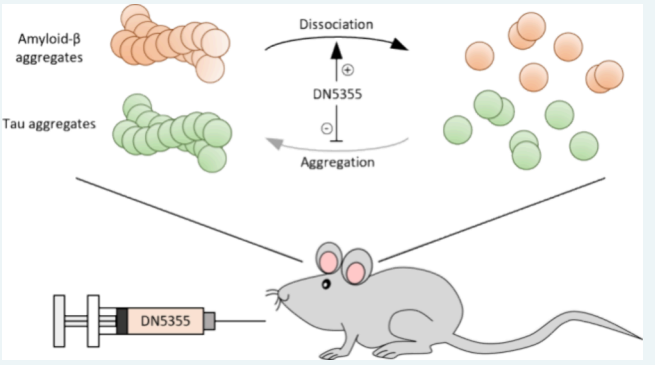

KEYWORDS: *Alzheimer's disease, amyloid-β, tau, cognitive recovery, neurodegeneration*

Alzheimer's disease (AD) is the most common type of dementia with typical deposition of plaques and tangles in the brain upon the misfolding of amyloid-β (Aβ) and hyperphosphorylated tau, respectively.[1] Given that Aβ and tau abnormalities directly contribute to neuronal loss, synaptic dysfunction, neuroinflammation, atrophy, and cognitive impairments of AD, both proteins, separately, have been the major therapeutic targets of the disease-modifying drug discovery.[2−6] During the past three decades, AD drug discovery mostly focused on the prevention of production, phosphorylation, and aggregation of Aβ and tau by inhibiting the early pathological mechanisms of AD such as amyloid precursor protein processing, kinase-mediated tau phosphorylation, and protein misfolding.[7−9] Failures of these approaches in clinical trials have provided lessons that clearance of preformed protein aggregates in the patient brain would have more therapeutic potentials as inhibition of the aforementioned pathology is better fit for preventive treatments.[10−12] Intravenous injection of antibodies targeting oligomers, protofibrils, and plaques of Aβ successfully reduced amyloid burden in brains of AD patients and partially slowed the progression of cognitive decline.[13,14] The disappointing cognitive benefit of anti-Aβ antibodies is still in debate, probably due to the weaker association of Aβ plaques with neurodegeneration in comparison to that of tau abnormalities.[15] Anti-tau antibody drug candidates have not shown significant tangle reduction and cognitive benefits yet, as intraneuronal tau is more difficult to access than extracellular Aβ.[16] Although antibodies possess outstanding therapeutic potentials in clearance of misfolded proteins, issues of low blood−brain barrier (BBB) penetration and the non-oral administration route remain to be solved.[17,18]

Our aim in this study was to design a new chemical entity directly targeting and dissociating aggregates of both Aβ and tau and to assess its therapeutic functions in *in vitro* and *in vivo* models of AD. Here, we synthesized 52 novel chemical derivatives (DN series) of necrostatin-1 (Nec-1), which we previously repurposed for an Aβ and tau dual targeting molecule from necroptosis inhibitor. Then, we conducted screening assays to identify chemicals with high efficacies in inhibiting Aβ aggregation and dissociating preformed Aβ fibrils *in vitro*. We investigated the efficacy of the selected chemicals in inhibiting tau aggregation and disrupting pre-existing tau aggregates. Thioflavin T (ThT), a fluorescent dye known for

Received: January 8, 2024
Revised: June 4, 2024
Accepted: June 11, 2024
Published: June 26, 2024

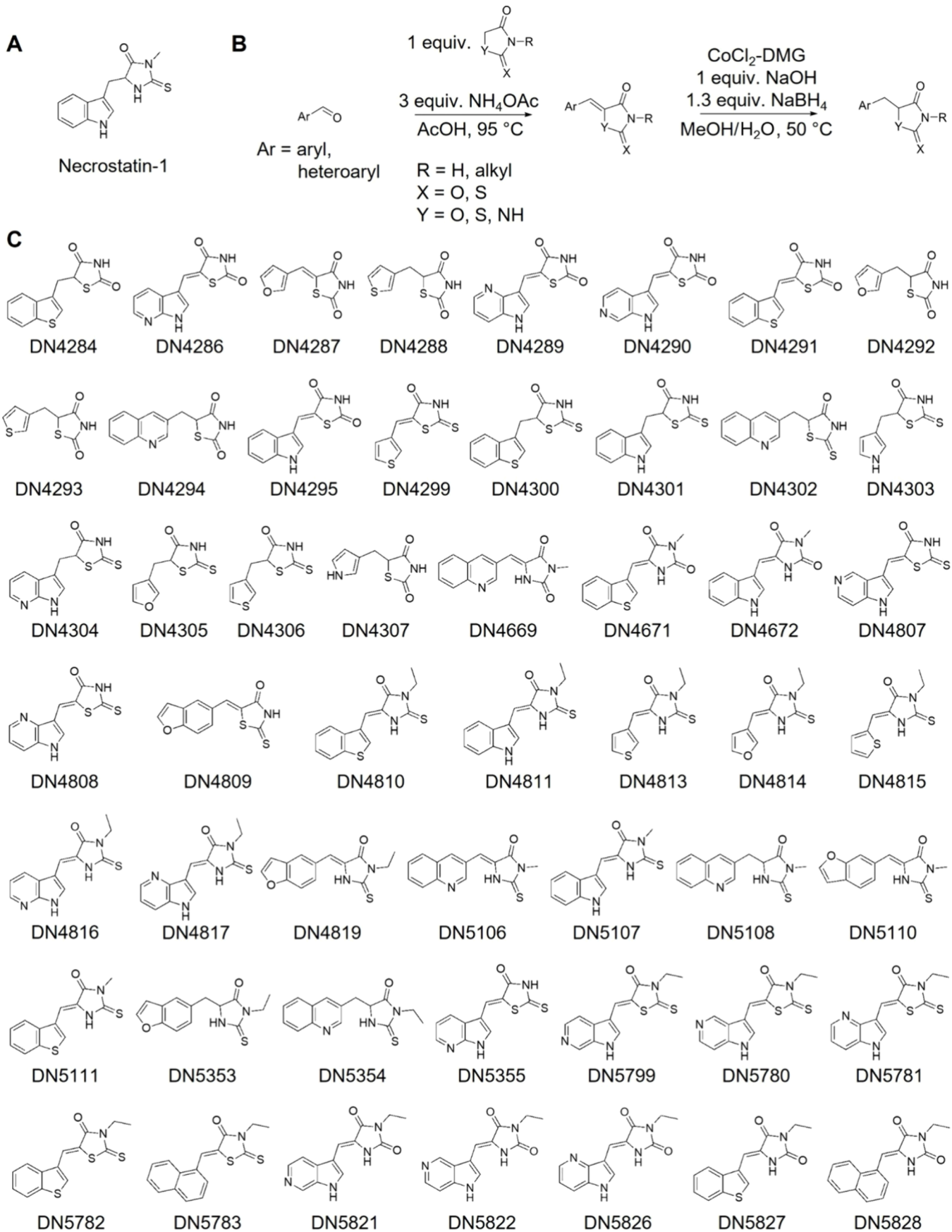

Figure 1. Synthesis of DN chemical library. (A) Structure of Nec-1. (B) General synthesis scheme. (C) Structures of the synthesized DN compounds. equiv., equivalent

https://doi.org/10.1021/acsptsci.4c00006
ACS Pharmacol. Transl. Sci. 2024, 7, 2650−2661

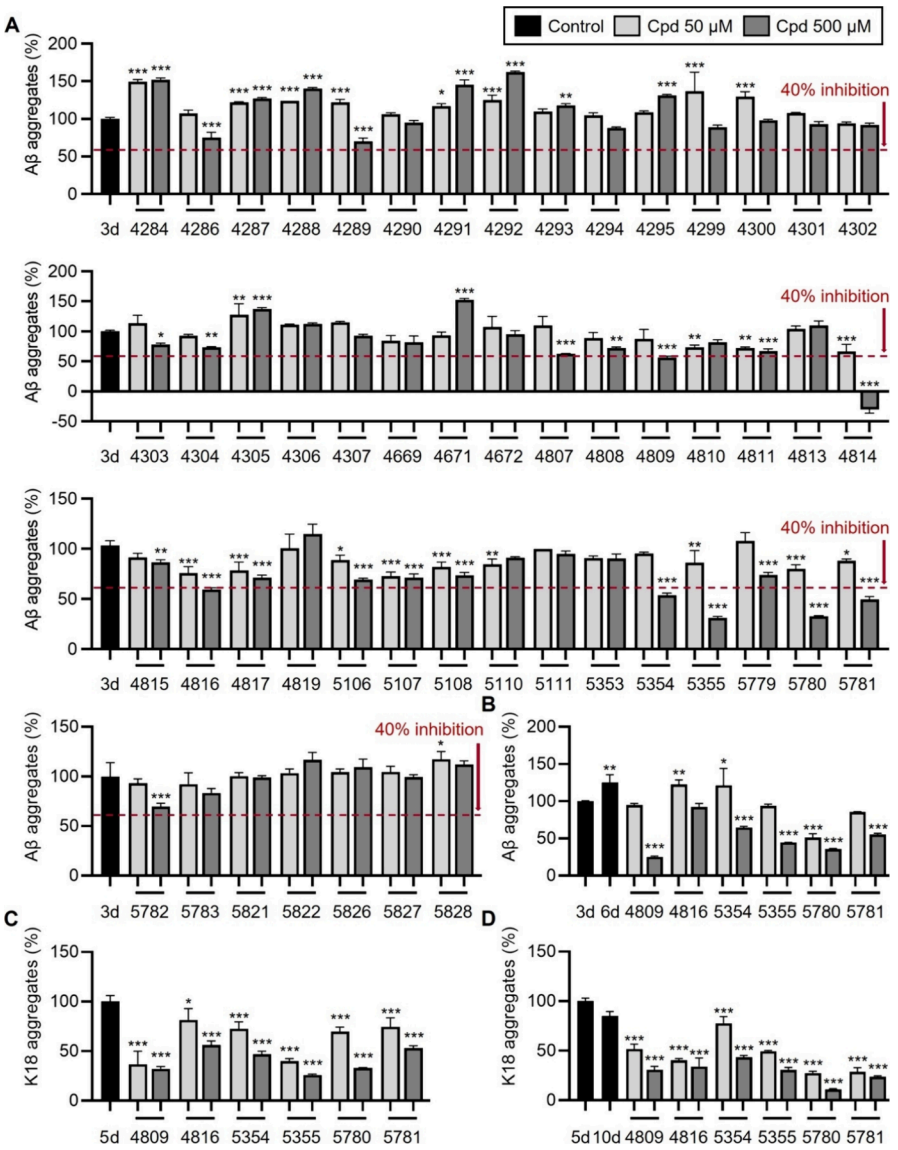

Figure 2. ThT fluorescence-based protein quantification for Aβ and tau aggregates. (A) Aβ aggregation inhibition assay. 50 and 500 μM of DN compounds were individually incubated with Aβ (25 μM) for 3 days at 37 °C. Data are normalized to 3-day incubated Aβ aggregates (3d, 100%). Red dotted line indicates the 40% inhibition of Aβ aggregation. (B) Aβ fibril dissociation assay with 6 selected DN compounds. Following a 3-day incubation for Aβ fibril formation, Aβ (25 μM) was individually incubated with the selected compounds (50 and 500 μM) for an additional 3 days at 37 °C. Data are normalized to the 3-day incubated Aβ control (3d, 100%). (C) Tau aggregation inhibition assay with 6 selected DN compounds. Each DN compound (50 and 500 μM) was incubated with K18 (35 μM) for 5 days at 37 °C. Data are normalized to 5-day incubated K18 aggregates (5d, 100%). (D) Tau fibril dissociation assay with 6 selected DN compounds. After 5 days of incubation to generate tau fibrils, K18 (35 μM) was further individually incubated with the selected DN compounds (50 and 500 μM) for an additional 5 days at 37 °C. Data are normalized to the 5-day incubated K18 control (5d, 100%). To measure the amount of aggregated proteins, ThT (5 μM) was added, and the fluorescence intensities were measured ($\lambda_{ex}/\lambda_{em}$ = 450 nm/485 nm). All data are presented as means ± standard deviation (SD). *p < 0.05, **p < 0.01, and ***p < 0.001 vs 3d control for Aβ and 5d control for K18; other comparisons were not significant (one-way analysis of variance (ANOVA) followed by Bonferroni's *post-hoc* comparisons tests); 3d, 3-day incubated Aβ; 6d, 6-day incubated Aβ; 5d, 5-day incubated K18; 10d, 10-day incubated K18; Cpd, compound.

its binding to and quantification of β-sheet structures, was utilized to assess aggregate levels in both Aβ and tau screening assays.[19] We selected DN5355 as a promising dual-targeting drug candidate capable of modulating aggregation of both Aβ and tau as well as dissociating preformed aggregates. A comparative analysis between DN5355 and Nec-1 was conducted to evaluate the efficacy of Aβ and tau aggregation using the ThT assay. Prior to *in vivo* therapeutic evaluations, we examined the ability of DN5355 to cross the BBB using a parallel artificial membrane permeability assay (PAMPA) and conducted metabolic profile analyses. Additionally, the interaction of DN5355 with Aβ was studied using a mapping Aβ plate (MAP) assay, and a fluorometric method was employed to explore the interaction of DN5355 with monomeric and aggregated tau.[20,21] Subsequently, the therapeutic efficacy of DN5355 was assessed in the 5XFAD (B6SJL-Tg(APPSwFlLon,PSEN1*146L*L286V)-6799Vas/Mmjax) transgenic mouse model of AD through behavioral and pathophysiological analyses. Following the administration of DN5355, learning and memory performance

https://doi.org/10.1021/acsptsci.4c00006
ACS Pharmacol. Transl. Sci. 2024, 7, 2650−2661

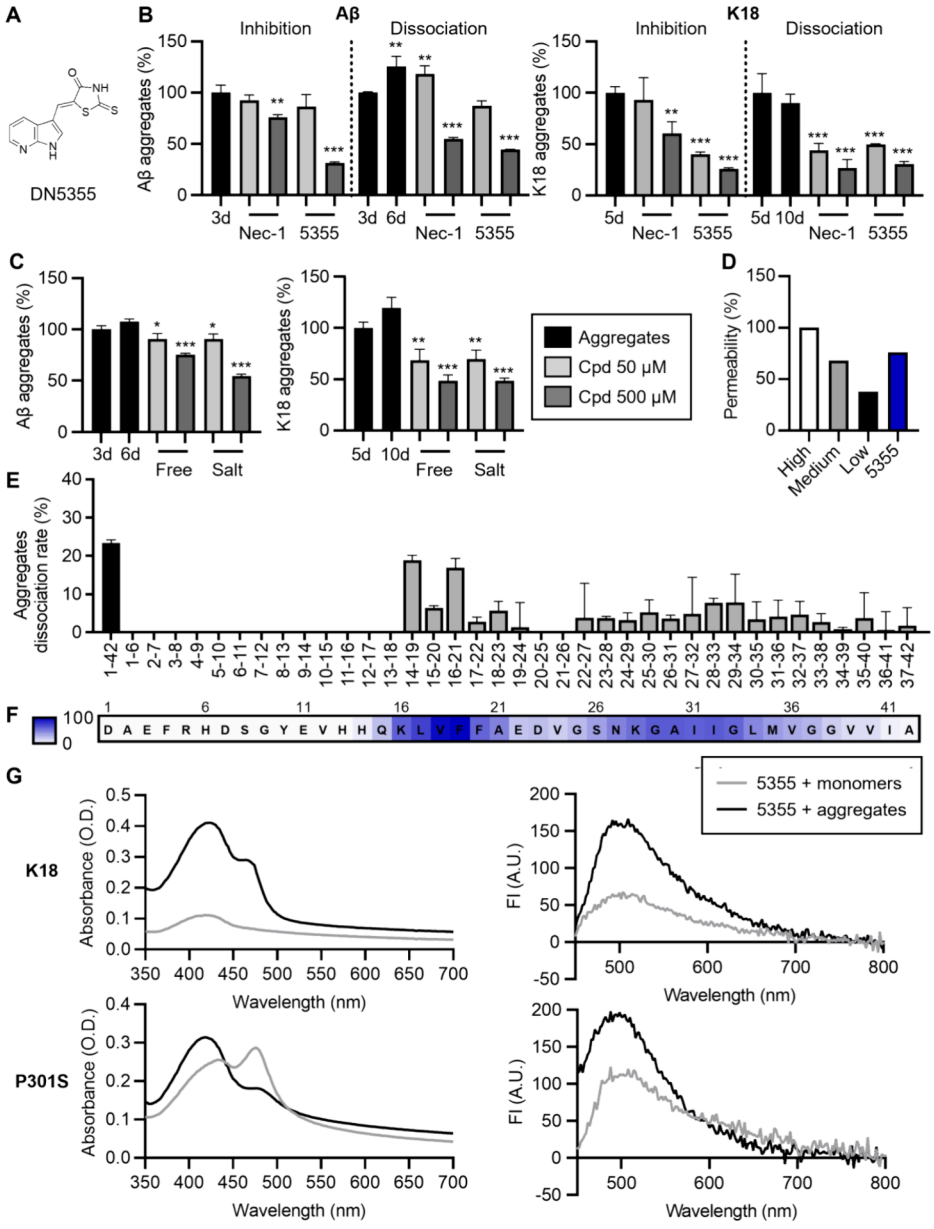

Figure 3. *In vitro* evaluation of DN5355 and interaction of DN5355 with Aβ or tau. (A) Chemical structure of DN5355. (B) Comparison of Aβ and tau aggregation inhibition and aggregate dissociation assays with Nec-1 and DN5355. Data are normalized to 3-day incubated Aβ control (3d, 100%) or 5-day incubated K18 control (5d, 100%). (C) Aβ and tau disaggregation assays with free and salt forms of DN5355. Data are normalized to 3-day incubated Aβ (3d, 100%) or 5-day incubated K18 controls (5d, 100%). (D) BBB-PAMPA test of DN5355. Data are normalized to the high-permeability control (100%). (E) MAP assay to discover the Aβ-interacting site of DN5355 that leads to Aβ fibril dissociation. (F) Heatmap of the dissociation rate by MAP assay (white to blue, 0 to 100%). (G) DN5355-tau binding assay utilizing K18 or P301S. Each tau was treated with 100 μM DN5355 as monomers (non-incubated tau) or as aggregates (5-day incubated K18 or P301S at 35 μM). The absorbance of DN5355 was scanned from 350 to 700 nm and used for a subsequent fluorescence spectrum scan at an excitation of 420 nm. All data are presented as mean ± SD; *p < 0.05, **p < 0.01, and ***p < 0.001 vs 3d control for Aβ and 5d control for K18; other comparisons were not significant (one-way ANOVA followed by Bonferroni *post-hoc* comparison); 5355, DN5355; 3d, 3-day incubated Aβ; 6d, 6-day incubated Aβ; 5d, 5-day incubated K18; 10d, 10-day incubated K18; Cpd, compound; P301S, tau with P301S mutation; FI, fluorescence intensity.

were assessed using the Y-maze spontaneous alteration test and contextual fear conditioning (CFC) test. Immunohistochemistry was utilized to evaluate Aβ plaques, while immunoblotting was employed to analyze total tau and phosphorylated tau proteins.[22,23]

RESULTS AND DISCUSSION

Synthesis of DN Chemical Library. The molecular structure of Nec-1 is composed of two moieties: an indole and a thiohydantoin (Figure 1A). Given its capability to modulate both Aβ and tau proteins, we prepared a chemical library of Nec-1 derivatives possessing a structure incorporating a heteroaryl group and a hydantoin-based group. The library includes 52 DN chemicals synthesized through Knoevenagel condensation of aldehydes and diones aimed at assessing their therapeutic potential in targeting Aβ and tau (Figure 1B,C). Additionally, the chemical diversity was extended by the synthesis of single-bond Knoevenagel adducts

https://doi.org/10.1021/acsptsci.4c00006
ACS Pharmacol. Transl. Sci. 2024, 7, 2650−2661

using a $CoCl_2$-dimethylglyoxime (DMG)-mediated reduction reaction.

Screening of Chemicals against Aβ and Tau Aggregation. Our primary goal of our study has been to identify chemicals that target both Aβ and tau proteins. Since the accumulation of Aβ is an early event in AD, we initially performed the fluorescence-based protein assay focused on Aβ aggregation inhibition and narrowed down the drug candidate. Subsequently, we conducted an assay to target Aβ aggregate dissociation with selected compound followed by the tau protein aggregation inhibition assay and aggregate dissociation assay. To measure the levels of Aβ and tau aggregates in assays, we utilized ThT that binds to and quantifies β-sheet structures.[19] For the primary screening, monomeric Aβ (25 μM) was incubated with each of 52 DN compounds (50 and 500 μM) for 3 days at 37 °C, followed by the addition of ThT solution to quantify Aβ fibrils. We found six hit compounds (DN4809, DN4816, DN5354, DN5355, DN5780, and DN5781) which significantly inhibited Aβ aggregation by more than 40% at 500 μM in comparison to the 3 day incubated Aβ control without compounds (Figure 2A). DN5355 and DN5780, in particular, reduced the level of Aβ aggregation by up to 70% of the control. DN4814 was excluded due to its high background fluorescence signal, which could interfere with the accurate measurement of Aβ fibrils and potentially confound the results.

Since Aβ aggregates can act as seeds for generating toxic Aβ aggregates further, therapeutic approaches that remove pre-existing Aβ plaques and halt ongoing aggregation will be highly effective in impeding disease progression.[24,25] Therefore, we evaluated the efficacy of the hit compounds in dissociating preformed Aβ aggregates. The monomeric Aβ was incubated at 37 °C for 3 days to obtain fibrils, which were then incubated with each DN compound for an additional 3 days at 37 °C to induce dissociation of Aβ fibrils. All hit compounds significantly dissociated preformed Aβ fibrils when treated at 500 μM (Figure 2B).

We additionally conducted a ThT assay to evaluate the efficacy of six hit compounds in inhibiting the aggregation of tau and dissociating tau fibrils. To investigate tau−tau interaction and aggregation, we employed tau K18 (K18), a recombinant human tau fragment containing four repeat domains of human tau.[26] For the tau aggregation inhibition assay, we incubated freshly prepared K18 monomers with 50 or 500 μM of the six hit compounds at 37 °C for 5 days. Co-incubation of tau monomers with each compound at both 50 and 500 μM distinctly prevented tau fibril formation in comparison to the non-treated 5-day incubated tau control (Figure 2C). Furthermore, all hit compounds significantly dissociated tau fibrils that were prepared by pre-incubation at 37 °C for 5 days, compared to the 5-day incubated tau control (Figure 2D).

Through the inhibition and dissociation assays, we discovered that DN4809, DN4816, DN5354, DN5355, DN5780, and DN5781 not only effectively inhibit both Aβ and tau aggregation but also dissociate pre-existing fibrils of both proteins. Notably, DN5355 and DN5780 exhibited remarkable inhibitory effects on Aβ aggregation, reducing total aggregates by 68.68% and 67.20%, respectively, at 500 μM, while DN4809 significantly dissociated preformed Aβ fibrils by 74.68%. Among the tested compounds, DN5355 demonstrated the strongest inhibitory effect on tau aggregation, reducing it by 74.12%, while DN5780 showed greater efficacy in dissociating pre-existing tau aggregates, at 89.16%. Based on its efficacy and patentability, we selected DN5355 as the compound with the highest novelty and effectiveness in inhibiting and reversing both Aβ and tau aggregations, making it a suitable candidate for further investigation.

Evaluation of DN5355 to Assess Drug Compatibility. Prior to further experiments, additional assays were conducted to compare the efficacy of DN5355 and Nec-1 modulating Aβ and tau. DN5355 exhibited superior effectiveness compared to Nec-1 in inhibiting and reversing Aβ aggregation as well as inhibiting tau fibril formation (Figure 3B). Subsequently, we investigated whether the salt form of DN5355, employed for improved aqueous solubility, maintained therapeutic efficacy comparable to the free form. Both forms showed similar effects on tau aggregate dissociation with the salt form demonstrating enhanced efficacy in dissociating Aβ aggregates (Figure 3C). Next, the BBB permeability of DN5355 was assessed, a critical consideration for drugs targeting brain proteins.[27] PAMPA results revealed that the permeability level of DN5355 is slightly higher compared to that of the medium permeability controls, implying sufficient BBB penetration of DN5355 (Figure 3D).

Interactions of DN5355 with Aβ and Tau. To investigate the interaction between DN5355 and Aβ, we utilized a MAP assay to identify the Aβ-binding site of DN5355.[20] We immobilized full-length Aβ or 6-amino-acid long Aβ fragments in a maleimide plate and added Flamma 552-tagged Aβ peptides (Fl-Aβ), which allowed the immobilized Aβs to aggregate for 6 h at 37 °C. To dissociate the interaction between immobilized Aβ fragments and Fl-Aβ, DN5355 was treated at a concentration of 500 μM in each well. The mixture was left to incubate at room temperature for 1 day. Fluorescence intensities of Fl-Aβ were measured both before and after treatment with DN5355, with post-treatment data normalized to pre-treatment levels using full-length Aβ as a control. The fluorescence intensities of the Aβ(16-21) fragment closely resembled those of monomeric Aβ, suggesting that binding of DN5355 to the KLVFFA domain induces dissociation of Aβ aggregates (Figure 3E,F). The KLVFFA domain, an amyloidogenic segment of Aβ characterized by its high hydrophobicity, has demonstrated potential in disrupting Aβ fibril formation through peptide mimetics. This underscores the critical role of DN5355 binding to this region in promoting the dissociation of Aβ fibrils.[28−31]

Furthermore, we delved into the interaction of DN5355 with tau proteins. In addition to K18, we utilized the P301S mutant tau variant (P301S), a widely studied tau isoform associated with early onset frontotemporal dementia and other tauopathies.[32−34] Monomeric and aggregated forms of each tau were prepared, with aggregated forms generated by incubating K18 or P301S for 5 days at 37 °C. Both monomeric and aggregated K18 or P301S were individually treated with 100 μM of DN5355, after which absorbance and fluorescence spectra were measured. We observed a noticeable enhancement in the fluorescence signal of DN5355-treated tau aggregates in comparison to that of the DN5355-treated monomeric tau, demonstrating the structural specificity of DN5355 in interacting with the aggregated forms of both tau proteins (Figure 3G). In addition, the observed changes in absorbance following DN5355 treatment, characterized by a notable increase in K18 aggregates and a shift in the primary absorbance peak of P301S monomers from 480 to 420 nm,

https://doi.org/10.1021/acsptsci.4c00006
ACS Pharmacol. Transl. Sci. 2024, 7, 2650−2661

Table 1. Pharmacokinetic Profiling of DN5355[a]

	Metabolic Stability (%)			Plasma Stability (%)			
				Human		Rat	
Compound	Human	Rat	Mouse	30 min	120 min	30 min	120 min
DN5355	21.0	45.7	9.5	>100	>100	96.4	>100
Control	13.7			>100	94.7	25.0	<1

	CYP Inhibition (%)				
Compound	CYP1A2	CYP2C9	CYP2C19	CYP2D6	CYP3A4
DN5355	57.5	84.2	85.6	89.6	94.5
Control	>100	97.4	>100	99.7	30.3

[a]Control: verapamil for metabolic stability, enalapril for plasma stability, and ketoconazole for CYP450 inhibition assay.

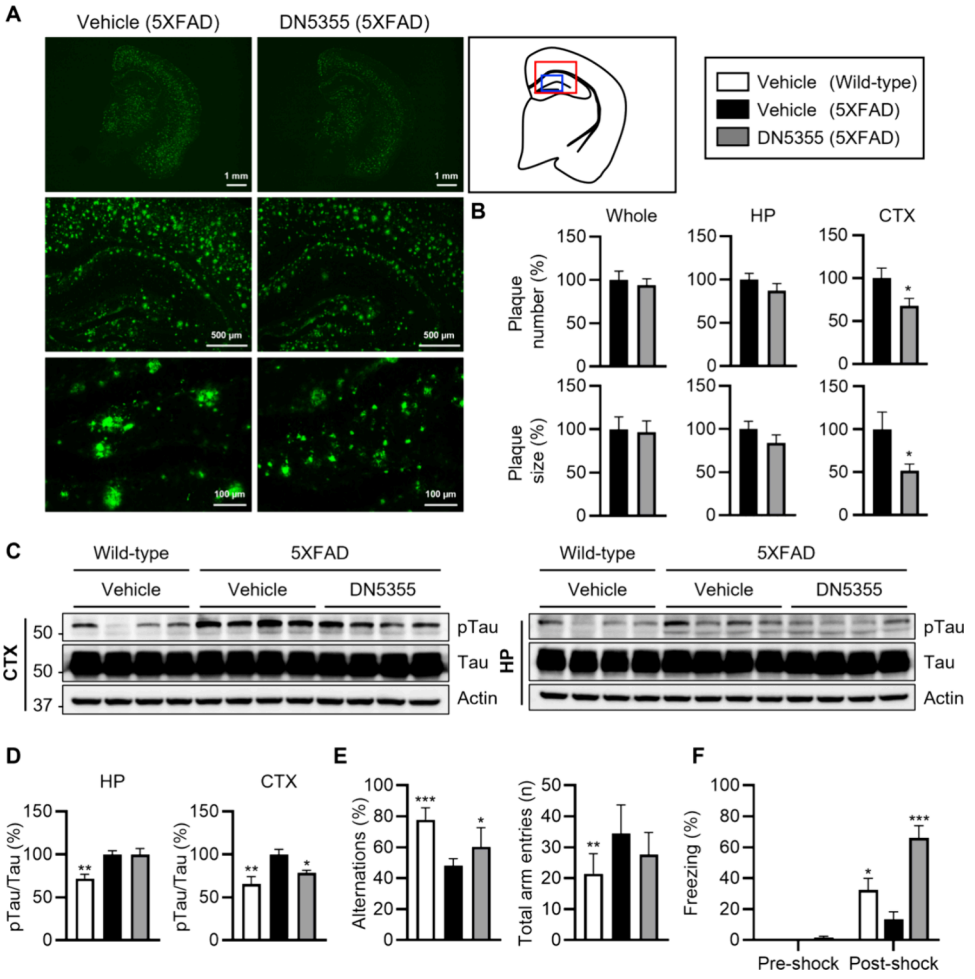

Figure 4. Therapeutic effects of 10-week DN5355 treatment in 8-month-old 5XFAD. (A) Representative immunohistochemical images display Aβ plaques stained with anti-Aβ antibody (D54D2) in vehicle or DN5355 treatment. The brain illustration with red and blue boxes on the right indicates the magnified brain regions imaged. Scale bars = 1 mm, 500 μm, and 100 μm. (B) % Number and size of Aβ plaques in the whole hemisphere, hippocampus, and cortex (n = 8 each). Data are normalized to vehicle-treated 5XFAD (100%) and presented as mean ± SD, *p < 0.05 vs vehicle-treated 5XFAD control; other comparisons were not significant (student's t test). (C) Immunoblot and (D) densitometry analysis of phosphorylated tau and total tau expression levels in hippocampus and cortex (n = 8 each). (E) % Alternations and total arm entries in the Y-maze spontaneous alternation test and (F) % freezing before (pre-shock) and after (post-shock) foot shocks at 0.3 mA in the CFC test executed on the ninth and 10th weeks of administration, respectively. Vehicle-treated wild-type (n = 13), vehicle-treated 5XFAD (n = 8), and DN5355-treated 5XFAD (n = 8) mice were used. Data are presented as mean ± SD, *p < 0.05, **p < 0.01, and ***p < 0.001 vs vehicle-treated 5XFAD controls; other comparisons were not significant (one-way ANOVA followed by Bonferroni *post-hoc* comparisons). HP, hippocampus; CTX, cortex; Actin, β-actin; pTau, phosphorylated tau.

indicate a direct interaction between DN5355 and the tau proteins.

We evaluated the pharmacokinetic properties of DN5355, specifically focusing on metabolic and plasma stabilities as well as cytochrome P450 (CYP) inhibition rates (Table 1). In metabolic stability assays using liver microsomes, DN5355 exhibited rapid liver metabolism, with a half-life of less than 30 min, employing verapamil as a control. On the other hand,

https://doi.org/10.1021/acsptsci.4c00006
ACS Pharmacol. Transl. Sci. 2024, 7, 2650−2661

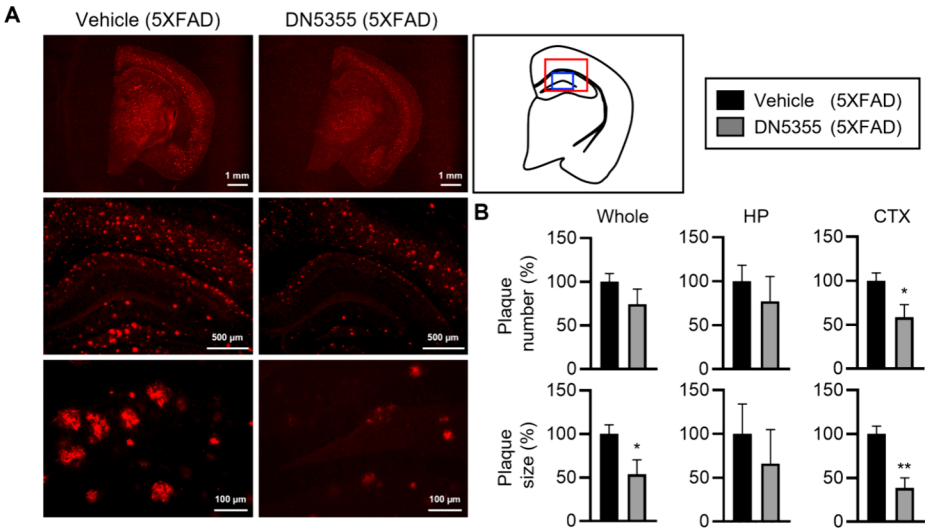

Figure 5. Therapeutic effect of DN5355 on the Aβ plaque burden in 6-month-old 5XFAD transgenic mice. (A) Representative images of 6E10-positive Aβ plaques in vehicle- or DN5355-treated 6-month-old male 5XFAD mice after 6 weeks of treatment. The brain scheme on the right with red and blue boxes indicates the magnified brain regions imaged. Scale bars = 1 mm, 500 μm, and 100 μm. (B) Plaque number and size in the whole hemisphere, hippocampus, and cortex (n = 5 each). Quantified data are normalized to vehicle-treated 5XFAD mice (100%) and are presented as mean ± standard error of the mean. *p < 0.05 and **p < 0.01 vs vehicle-treated 5XFAD controls; other comparisons were not significant (student's t test). HP, hippocampus; CTX, cortex.

plasma stability tests in human and rat plasma indicated that DN5355 maintained stability for up to 2 h, with enalapril serving as the control. Additionally, the assessment of CYP450 inhibition rates showed minimal inhibition across most CYP enzymes, except for CYP1A2, which displayed a significant inhibition rate of approximately 40% in comparison to the control, ketoconazole.

Long-Term Administration of DN5355 to 5XFAD Mice. With the established inhibitory effects of DN5355 on Aβ and tau aggregations and its proven capacity to reverse Aβ and tau aggregates *in vitro*, we sought to investigate the potential of DN5355 to ameliorate cognitive impairments associated with Aβ plaques and neurofibrillary tangles. Utilizing the 5XFAD mouse model, which exhibits rapid Aβ plaque accumulation starting at two months, peaking at six months, and a corresponding increase in phosphorylated tau levels by six months, reflecting key aspects of AD pathology, we administered DN5355 to 8-month-old male 5XFAD mice (n = 8) via drinking water at a dosage of 50 mg/kg/day for a duration of 10 weeks.[23,35,36] In this study, vehicle-treated wild-type mice (n = 13) and 5XFAD mice (n = 8) were included as control groups for comparative analysis. To assess short-term spatial memory, a Y-maze spontaneous alternation test was conducted in the ninth week of administration, calculating the percentage of alternations. DN5355-treated mice exhibited improved spatial memory deficits compared to those of vehicle-treated 5XFAD mice (Figure 4E). The effect of DN5355 on associative learning was evaluated during the last week of administration using a CFC test. DN5355 treatment significantly enhanced the performance of 5XFAD mice in the CFC test, suggesting improved associative learning abilities (Figure 4F). Following the behavioral tests, brain samples were collected for immunohistochemical analysis and immunoblotting assays to evaluate changes in the pathological protein levels. Notably, visualization through immunohistochemistry showed that DN5355 administration led to a reduction in both the number and size of Aβ plaques specifically in the cortex (Figure 4A,B). Given the established association between the burden of tau aggregates in the brain and cognitive decline in AD patients from previous reports, we conducted immunoblotting analysis of tau phosphorylation in the hippocampal and cortical lysates obtained from vehicle- and DN5355-treated mice.[37−39] Remarkably, reduced levels of phosphorylated tau were observed in the cortex of DN5355-treated 5XFAD mice in comparison with the vehicle-treated 5XFAD controls (Figure 4C,D). These findings highlight the potential of DN5355 in modulating both Aβ and tau pathologies *in vivo*, thereby leading to the amelioration of cognitive impairment in aged 5XFAD mice. Furthermore, the enhancement in cognitive deficits observed in DN5355-treated mice indicates that the dissociation of Aβ plaques facilitated by DN5355 did not lead to the formation of harmful toxic Aβ oligomers.

Short-Term Administration of DN5355 to 5XFAD Mice. To evaluate if comparable therapeutic effects to those observed in 8-month-old 5XFAD mice could be achieved with a lower concentration and shorter treatment duration, DN5355 was administered to 6-month-old 5XFAD mice via drinking water at a dosage of 30 mg/kg/day for 6 weeks (n = 5). A control group consisting of vehicle-treated 5XFAD mice was employed for comparison (n = 5). After 6 weeks of administration, brain tissues were collected for histochemical analysis. In mice treated with DN5355, a notable reduction in Aβ plaques was observed within the brain, particularly in the cortical region, where a significant decrease was noted compared to the vehicle-treated group (Figure 5A,B). These findings collectively demonstrate that the administration of DN5355 at a dosage of 30 mg/kg/day for 6 weeks resulted in the effective removal of Aβ plaques in the brains of 5XFAD mice.

Interestingly, the DN5355 treatment resulted in significant reductions in both the number and size of Aβ plaques in 6-month-old 5XFAD mice (approximately 25% and 46% reductions, respectively) compared to their 8-month-old counterparts (approximately 11% and 17%, respectively), despite the lower dosage and shorter treatment period. This

https://doi.org/10.1021/acsptsci.4c00006
ACS Pharmacol. Transl. Sci. 2024, 7, 2650−2661

difference may be due to the varying levels of Aβ plaque compactness in the brain between the two age groups. To achieve a comparable level of plaque clearance as in 6-month-old 5XFAD mice, a higher dose of DN5355 may have been required for more densely aggregated Aβ plaques in 8-month-old 5XFAD mice.

The reductions of Aβ plaque and tau phosphorylation varied between the cortex and hippocampus, with the cortex appearing to be more affected by DN5355 administration. DN5355 may have a discrete distribution pattern across the cortical and hippocampal regions, which could explain the discrepancies observed. To better understand this, it is necessary to investigate the drug's distribution in specific brain regions.[40] Future investigations should focus on elucidating why the hippocampal region, which is closely linked to long-term memory and AD-related cognitive symptoms, demonstrated less pronounced effects of DN5355 treatment.[41,42]

The approval by the Food and Drug Administration of monoclonal antibodies that target Aβ highlights the significance of Aβ in the development of AD.[43] However, their ability to reverse cognitive decline remains uncertain, despite their ability to reduce Aβ plaques and slow disease progression.[14,44] Given the strong association between cognitive decline and tau accumulation, targeting tau in addition to Aβ remains imperative for a complete resolution of AD.[45] Small molecule drugs provide a competitive advantage due to their ability to cross the BBB and target intracellular aggregates through modification of chemical properties such as lipophilicity, charge, and size.[46−48] Based on our findings, we expect that DN5355 can serve as a structural motif for the development of small molecule drugs targeting both Aβ and tau, simultaneously.

The promising efficacy of DN5355 in ameliorating cognitive decline through oral administration highlights its potential for developing safe oral drug formulations, which can improve patient compliance and provide cost-effective treatment options to a broader spectrum of individuals. Further research is needed to understand DN5355's distribution in the brain, identify optimal dosages and treatment durations, and unravel the structural mechanisms affecting Aβ and tau aggregates. These insights are crucial for enhancing structural strategies in the discovery of small molecules for AD, paving the way for more targeted therapeutic interventions with potential disease-modifying effects.

CONCLUSION

Through screening 52 Nec-1 derivatives, we identified DN5355 as a potent chemical capable of inhibiting and reversing Aβ and tau aggregation *in vitro*. DN5355 can cross the BBB and directly interact with Aβ and tau aggregates, resulting in therapeutic benefits in 8-month-old 5XFAD mice by reducing cortical Aβ plaques, tau phosphorylation, and cognitive deficits, as well as significantly reducing endogenous Aβ plaques in 6-month-old 5XFAD mice. DN5355 represents a promising small molecule therapeutic targeting Aβ and tau proteins, providing advancements in neurodegenerative disease research.

METHODS

Animal. 5XFAD mice were obtained from the Jackson Laboratory and were maintained by mating with (C57BL/6 x SJL)F1 mice. The genotype of the mice was confirmed by polymerase chain reaction (PCR) analysis of tail DNA prior to administration using the standard PCR conditions from Jackson Laboratory. All mice were housed in a laboratory animal breeding room at Yonsei University and maintained under controlled temperature and humidity with an alternating 12-h light-dark cycle and access to food and water *ad libitum*.

All animal experiments were performed in accordance with the National Institutes of Health guidelines for the care and use of laboratory animals. The animal experiment protocols were approved by the Institutional Animal Care and Use Committee of Yonsei University (IACUC-202107-1300-01).

Chemical Syntheses of Nec-1 Derivatives. For the synthesis of Nec-1 derivatives, aldehyde (3 mmol) and dione (1.0 equiv) were added to 3 mL of acetic acid. The mixture was stirred at room temperature, and ammonium acetate (3.0 equiv) was added dropwise to the reaction solution. The temperature was gradually increased to 95 °C, and the solution was stirred for 2 h. The resulting product was filtered to obtain crystals and purified by recrystallization in hexane and ethyl acetate. The completion of the reaction was confirmed through thin-layer chromatography. For the $CoCl_2$-DMG mediated reduction of synthesized compound, 0.5 mmol of compound was dissolved in a mixed solvent (1 mL) of methanol and water (1:1.5, v/v). Sodium hydroxide (1.0 equiv) was added dropwise at room temperature, and the solution was stirred for 15 min. 42 mg of cobalt chloride and 250 mg of DMG were prepared in 5 mL of dimethylformamide, and 30 μL of the mixture was added to the reaction solution, followed by stirring at room temperature for an additional 15 min. Then, sodium boron hydroxide (1.3 equiv) was added and stirred at 50 °C for 24 h. After the completion of the reaction, the reaction solution was cooled to room temperature. The reaction was terminated with water, and ethyl acetate was further added to extract the product. The organic layer was washed with brine and dehydrated with sodium sulfite. The residue was obtained by distilling the solvent under reduced pressure and was purified by high-performance liquid chromatography.

ThT Fluorescence Assays. For ThT assays with Aβ, Aβ peptides were synthesized using solid-phase peptide synthesis as previously reported.[49] Synthetic Aβ and Nec-1 derivatives were dissolved in dimethyl sulfoxide (DMSO) (Sigma-Aldrich, no. D8418) as 10 mM stock. For the evaluation of Aβ aggregation inhibition by Nec-1 derivatives, Aβ (25 μM) was incubated with the compounds (50 and 500 μM) at 37 °C for 3 days. In the Aβ fibril disaggregation assays, we generated Aβ fibrils by incubating Aβ (250 μM) for 3 days at 37 °C. Nec-1 derivatives were then treated and further incubated for 3 days at 37 °C, at final concentrations of 25 μM for Aβ and 50 and 500 μM for the derivatives. For ThT assays with tau, recombinant human tau K18 fragments were dissolved in phosphate-buffered saline as a 1 mg/mL stock. K18 fragments (0.5 mg/mL) were coincubated with Nec-1 derivatives (50, 500 μM) at 37 °C for 5 days for tau aggregation inhibition assays. To induce tau fibrilization, heparin at 1 mg/mL (Sigma-Aldrich, #H3393) and dithiothreitol (DTT) at 100 μM (Tokyo Chemical Industry, #D1071) were used.[50] To assess the ability of DN5355 to reverse tau fibril formation, K18 fragments were incubated for 5 days at 37 °C to generate fibrils, then treated with 50 or 500 μM Nec-1 derivatives, and incubated for 5 days at 37 °C. After the incubation, 25 μL of incubated samples was transferred to a 96-well half-area black microplate (Corning, #3694), and 75 μL of 5 μM ThT

https://doi.org/10.1021/acsptsci.4c00006
ACS Pharmacol. Transl. Sci. 2024, 7, 2650−2661

solution (Sigma-Aldrich, #T3516) in 50 mM glycine buffer (pH 8.5) was added for the measurement of β-sheet-containing Aβ aggregates and tau fibrils. The fluorescence intensity of ThT binding on Aβ fibril or tau fibril was measured at 450 nm/485 nm (excitation/emission) using a multimode plate reader (Infinite M200 PRO, Tecan Life Sciences). To eliminate possible intervention of the fluorescence properties of DN compounds in the fluorescence readings, we deducted the fluorescence intensity of DN compounds without Aβ or K18 treatment from that of samples treated with Aβ or K18. Fluorescence intensity was normalized to that of incubated Aβ or K18 aggregates without Nec-1 derivatives (100%) as a control.

PAMPA Assay. Membrane permeability of DN5355 was tested using a PAMPA assay kit (BioAssay Systems, #PAMPA-096) according to the manufacturer's protocol. DN5355 and permeability controls were used at 50 μM in 10% DMSO.

Microsomal Stability Assay. Liver microsomes specific for human, rat, and mouse (Corning) were prepared in 0.1 M phosphate buffer (pH 7.4). DN5355 was added to be 1 μM in 0.5 mg/mL of microsome solution and pre-incubated for 5 min at 37 °C. Reaction was initiated by the addition of nicotinamide adenine dinucleotide phosphate (NADPH), and the mixture was incubated for 30 min at 37 °C. Acetonitrile (Sigma-Aldrich) containing 2 μM of chlorpropamide was added to terminate the reaction, and sample was spun down at 15,000 rpm, 4 °C for 5 min. The supernatant was loaded onto a liquid chromatography (LC)-mass spectrometry (MS)/MS system (TSQ Vantage, Thermo Fisher Scientific). Pre-incubated sample without NADPH was used as a control, and the microsomal stability of test compound was calculated as percent of control activity.

Plasma Stability Assay. Test compound was spiked into human or rat plasma (Biochemed) to be 10 mM and incubated at 37 °C for 0, 30, or 120 min with shaking. After incubation, 100 mL of each sample was transferred into a new 1.5 mL tube containing 200 mL of acetonitrile with 1 mM chlorpropamide as an internal standard. After vortexing the mixture, centrifugation at 15,000 rpm, 4 °C for 10 min was conducted to remove proteins and debris. The amount of tested compound in the sample was determined as an area ratio (area of analyte/area of internal standard) measured using the LC-MS/MS system. Stability data was presented as % remaining compared to control (0 min).

CYP Inhibition Assay. CYP inhibition was assessed by measuring the metabolites of CYP isoform specific substrates. A mixture of CYP specific probes (Sigma-Aldrich) containing 50 μM phenacetin, 10 μM diclofenac, 100 μM S-mephenytoin, 5 μM dextromethorphan, and 2.5 μM midazolam was prepared in 0.1 M phosphate buffer (pH 7.4) with 0.25 mg/mL human liver microsomes. In the mixture of microsome and probes, the test compound was added to be 10 μM and the sample was incubated for 5 min. The reaction was initiated by the addition of NADPH (Promega), and the mixture was incubated for 15 min at 37 °C. Acetonitrile containing 0.25 μM terfenadine as internal standard (Sigma-Aldrich) was added to terminate the reaction. After centrifugation of the reaction mixture at 15,000 rpm for 5 min at 4 °C, the supernatant was injected into the LC-MS/MS system. The reaction sample without the test compound was presented as control, and CYP enzyme activity was calculated as percent of control activity. All experiments were performed in duplicates.

MAP Assay. MAP assay was executed to identify the Aβ-binding site of DN5355 which is essential for the dissociation of Aβ aggregates.[20] MAP was prepared by immobilizing six-amino-acid-long Aβ fragments (5 μg), from Aβ1-6 to Aβ37-42, per well. An equal amount of full-length Aβ was immobilized as a control. In each well, 200 μL of cysteine (10 μg/mL) was treated for blocking non-specific binding, and each well was washed 3 times with wash buffer (0.1 M sodium phosphate, 0.15 M sodium chloride, 0.05% Tween 20, pH 7.2). Flamma 552-conjugated Aβ was treated in each well and incubated for 6 h at 37 °C to induce aggregation with fragmented Aβ. Wells were washed again with wash buffer, and DN5355 at 500 μM was added to each well, followed by a 24 h incubation at room temperature. Fluorescence intensities were measured at 550 nm/564 nm (excitation/emission) using a plate reader (SpectraMax M2e, Molecular Devices) after each washing step, and the aggregate dissociation rate (%) was calculated as [(Fluorescence intensity after incubation with DN5355 − Fluorescence intensity after incubation with Flamma 552-tagged Aβ)/(Fluorescence intensity before incubation with Flamma 552-tagged Aβ − Fluorescence intensity after incubation with Flamma 552-tagged Aβ)] × 100.

Tau Binding Fluorometric Assay. To evaluate the binding ability of DN5355 with different fragments of tau in monomeric and aggregated states, we utilized the K18 fragment and tau with P301S mutation. K18 or P301S peptides were incubated for 5 days at 37 °C with heparin (0.1 mg/mL) and DTT (100 μM) to generate aggregates. 100 μM of DN5355 was treated with incubated or non-incubated tau fragments, and the absorbance was measured at 2 nm increments from 350 to 700 nm in a 96-well clear round-bottom plate (Corning, #CLS3896). The solutions were then transferred to a 96-well black round-bottom plate (Greiner Bio-One, #650209), and the fluorescence was scanned from an excitation wavelength of 420 nm, as the excitation peak of DN5355 was detected at 420 nm. Fluorometric readings were performed using a multimode plate reader (Infinite M200 PRO, Tecan Life Sciences).

DN5355 Administration. To investigate the therapeutic potential of DN5355 *in vivo*, we treated 8-month-old male 5XFAD mice with vehicle (2% DMSO, 2% polyethylene glycol (PEG) 400, 0.4% NaOH; n = 8) or DN5355 (n = 8) at 50 mg/kg/day via *ad libitum* drinking water. Age-matched wild-type mice (n = 13) were administered with vehicle as controls. For the evaluation of DN5355 at a lower dosage and shorter treatment period, 6-month-old male 5XFAD mice were treated with vehicle (2% DMSO, 2% PEG400, 0.4% NaOH; n = 5) or DN5355 (n = 5) via *ad libitum* drinking water at 30 mg/kg/day for 6 weeks. For the administration of DN5355 at an exact dosage, daily water consumption of each cage was recorded and used for the calculation of the required amount of DN5355. Vehicle and DN5355 in vehicle were replaced every day.

Y-maze Test. Short-term spatial memory was evaluated by recording the spontaneous alternation behavior. The maze (Jeung Do Bio & Plant) was made of black plastic with three equally spaced arms (40 cm length, 10 cm width, 12 cm height). Visual cues were blocked by surrounding the maze with a black floor-to-ceiling curtain. Facing the end of the arm, each mouse was placed at the end of an arm and allowed to explore the maze freely for 8 min. An arm entry was defined as the mouse reaching the end of the arm, and all entries were manually recorded. To remove scent cues, the interior of the

https://doi.org/10.1021/acsptsci.4c00006
ACS Pharmacol. Transl. Sci. 2024, 7, 2650−2661

maze was cleaned with 70% ethanol and deionized water before testing each mouse. An alternation was defined as an entry to an arm not visited in the last two entries, and spontaneous alternation behavior was calculated as % alternation = [(number of alternations)/(total number of arm entries − 2)] × 100.

CFC Test. Following the Y-maze test, mice were allowed to rest for 2 days and handled for 1 to 2 min per day for 2 days before day 1 of CFC test. On the first day, the mice were individually placed in the chamber (Panlab, Harvard Apparatus) for 5 min for habituation. On day 2, each mouse was placed in the chamber and exposed to 0.3 mA foot shock for 2 s, twice at 178 and 238 s during the 5 min training phase. On the probe day, the mice were returned to the same chamber for 5 min without any foot shock. Time spent without any movement excluding respiratory movements in the chamber was automatically measured, and % freezing was automatically calculated with PACKWIN software (Panlab, Harvard Apparatus).

Immunostaining. All mice were sacrificed, and the brains were perfused with 0.9% NaCl before extraction. Collected brains were divided into hemispheres and used for immunoblotting or immunostaining. For immunostaining, the hemisphere was fixed in 4% paraformaldehyde (Biosesang, #P2031) and dehydrated in 30% sucrose for cryoprotection. 35-μm thick coronal sections were collected and stained with 6E10 (BioLegend, #SIG-39320) or D54D2 monoclonal antibodies (Cell Signaling Technology, #8243). Alexa Fluor 488- or 555-conjugated secondary antibodies (Invitrogen, #A28175, and #A27039) were utilized for fluorescence detection. Images were obtained using a Leica DM2500 microscope, and the number and sizes of plaques were measured with Image J.

Immunoblotting. Using the hemisphere of each mouse treated with vehicle or DN5355, we isolated the hippocampus and cortex. Isolated tissues were homogenized in radioimmunoprecipitation assay buffer (Sigma-Aldrich, #R0278) with protease (Sigma-Aldrich, #11836170001) and phosphatase inhibitors (Sigma-Aldrich, #04906845001) and then incubated on ice for 30 min, followed by centrifugation at 17,000 rpm at 4 °C for 30 min. The supernatant of each mouse was loaded on sodium dodecyl sulfate-polyacrylamide gel electrophoresis gels (25 μg/well) and transferred to nitrocellulose membranes (Bio-Rad, #1620112). The membranes were blocked with 5% milk (Difco, #232100) or bovine serum albumin (Sigma-Aldrich, #A3059) for 1 h at room temperature and then incubated with anti-tau (Abcam, #AB64193) or phosphorylated tau antibodies (Invitrogen, #MN1020) overnight at 4 °C. As a loading control, β-actin (Millipore Corporation, #MAB1501R) was used. The membrane was finally treated with horseradish peroxidase-conjugated secondary antibodies (anti-mouse: Bethyl Laboratories, #A90-116P; anti-rabbit: Jackson ImmunoResearch, #111-035-144dd). For detection, the membrane was developed with ECL solution (Thermo Fisher Scientific, #34580) following the manufacturer's instructions. The blot intensities were quantified with Image J.

Statistical Analysis. All data were organized into graphical data with Prism 9, and statistical analyses were conducted using one-way ANOVA followed by Bonferroni's *post-hoc* comparisons or student's *t* test (*p < 0.05, **p < 0.01, and ***p < 0.001).

■ ASSOCIATED CONTENT

Supporting Information

The Supporting Information is available free of charge at https://pubs.acs.org/doi/10.1021/acsptsci.4c00006.

^{1}H NMR data of synthesized compounds (PDF)

■ AUTHOR INFORMATION

Corresponding Authors

YoungSoo Kim − *Department of Pharmacy and Yonsei Institute of Pharmaceutical Science, Yonsei University, Incheon 21983, Republic of Korea; Department of Integrative Biotechnology and Translational Medicine, Yonsei University, Incheon 21983, Republic of Korea; Department of Psychiatry, Institute of Behavioral Science in Medicine, Yonsei University College of Medicine, Seoul 03722, Republic of Korea;* orcid.org/0000-0001-5029-7082; Email: y.kim@yonsei.ac.kr

Ki Bum Hong − *New Drug Development Center (NDDC), Daegu-Gyeongbuk Medical Innovation Foundation (KMEDIhub), Daegu 41061, Republic of Korea;* orcid.org/0000-0002-4853-2263; Email: kbhong@kmedihub.re.kr

Ji Hoon Lee − *New Drug Development Center (NDDC), Daegu-Gyeongbuk Medical Innovation Foundation (KMEDIhub), Daegu 41061, Republic of Korea;* Email: jhlee@dgmif.re.kr

Hye Yun Kim − *Department of Pharmacy and Yonsei Institute of Pharmaceutical Science, Yonsei University, Incheon 21983, Republic of Korea;* orcid.org/0000-0003-3757-5652; Email: hyeyunkim@yonsei.ac.kr

Authors

Sohui Park − *Department of Pharmacy and Yonsei Institute of Pharmaceutical Science, Yonsei University, Incheon 21983, Republic of Korea*

Jisu Shin − *Department of Pharmacy and Yonsei Institute of Pharmaceutical Science, Yonsei University, Incheon 21983, Republic of Korea*

Kyeonghwan Kim − *Department of Pharmacy and Yonsei Institute of Pharmaceutical Science, Yonsei University, Incheon 21983, Republic of Korea;* orcid.org/0000-0002-1681-8574

Darong Kim − *New Drug Development Center (NDDC), Daegu-Gyeongbuk Medical Innovation Foundation (KMEDIhub), Daegu 41061, Republic of Korea*

Won Seok Lee − *New Drug Development Center (NDDC), Daegu-Gyeongbuk Medical Innovation Foundation (KMEDIhub), Daegu 41061, Republic of Korea*

Jusuk Lee − *New Drug Development Center (NDDC), Daegu-Gyeongbuk Medical Innovation Foundation (KMEDIhub), Daegu 41061, Republic of Korea*

Illhwan Cho − *Department of Pharmacy and Yonsei Institute of Pharmaceutical Science, Yonsei University, Incheon 21983, Republic of Korea*

In Wook Park − *Department of Pharmacy and Yonsei Institute of Pharmaceutical Science, Yonsei University, Incheon 21983, Republic of Korea*

Soljee Yoon − *Department of Pharmacy and Yonsei Institute of Pharmaceutical Science, Yonsei University, Incheon 21983, Republic of Korea; Department of Integrative Biotechnology and Translational Medicine, Yonsei University, Incheon 21983, Republic of Korea*

Songmin Lee − *Department of Pharmacy and Yonsei Institute of Pharmaceutical Science, Yonsei University, Incheon 21983, Republic of Korea*

Complete contact information is available at: https://pubs.acs.org/10.1021/acsptsci.4c00006

Author Contributions

○S.P., J.S., K.K., and D.K. contributed equally. S.P. performed Aβ and tau ThT assays with the salt and free forms of DN5355, PAMPA, tau binding fluorometric assays, DN5355 administration, and behavior tests. J.S. performed *in vitro* Aβ and tau screening ThT assays of 52 Nec-1 derivatives and immunostaining assays of 6-month-old male 5XFAD mice treated with DN5355 at 30 mg/kg/day for 6 weeks. S.P. performed immunostaining and immunoblotting assays of 8-month-old male 5XFAD mice treated with DN5355 at 50 mg/kg/day for 10 weeks. I.C. performed MAP assay. K.K., I.W.P., and S.Y. synthesized Aβ; J.S. and S.L. prepared mice. Y.K. designed and supervised the study; S.P., J.S., and Y.K. analyzed the results. S.P., K.K., H.Y.K., K.B.H., J.H.L., and Y.K. wrote the manuscript.

Funding

This research was supported by the Korea Health Technology R&D Project (Grant Number: RS-2024-00349158) through the Korea Health Industry Development Institute (KHIDI) and Korea Dementia Research Center (KDRC), Republic of Korea, and Mid-Career Researcher Program (Grant Number: NRF-2021R1A2C2093916) and Basic Science Research Program (Grant Number: NRF-2018R1A6A1A03023718) through the National Research Foundation of Korea (NRF), funded by the Ministry of Health & Welfare and Ministry of Science and ICT, Republic of Korea.

Notes

The authors declare the following competing financial interest(s): Y.K. is an employee of Amyloid Solution and receives equity or equity options.

■ ACKNOWLEDGMENTS

All images were created by the authors of this manuscript, and all experimental protocols including animal tests in the article were approved by Yonsei University (IACUC-202003-1038-01) (NRF-2017M3A9G4052949). The authors thank Dr. Eunmi Hong from New Drug Development Center, Daegu Gyeongbuk Medical Innovation Foundation for providing us with K18 and P301S fragments of tau.

■ ABBREVIATIONS

AD, Alzheimer's disease; Aβ, amyloid-β; BBB, blood−brain barrier; CFC, contextual fear conditioning; CYP, cytochrome P450; K18, tau K18; MAP, mapping Aβ plate; Nec-1, necrostatin-1; P301S, tau with P301S mutation; PAMPA, parallel artificial membrane permeability assay; ThT, thioflavin T

■ REFERENCES

(1) Serrano-Pozo, A.; Frosch, M. P.; Masliah, E.; Hyman, B. T. Neuropathological alterations in Alzheimer disease. *Cold Spring Harb. Perspect. Med.* **2011**, *1* (1), a006189.

(2) Palop, J. J.; Mucke, L. Amyloid-beta-induced neuronal dysfunction in Alzheimer's disease: from synapses toward neural networks. *Nat. Neurosci.* **2010**, *13* (7), 812−818.

(3) Minter, M. R.; Taylor, J. M.; Crack, P. J. The contribution of neuroinflammation to amyloid toxicity in Alzheimer's disease. *J. Neurochem.* **2016**, *136* (3), 457−474.

(4) Bloom, G. S. Amyloid-β and tau: the trigger and bullet in Alzheimer disease pathogenesis. *JAMA Neurol* **2014**, *71* (4), 505−508.

(5) Muralidar, S.; Ambi, S. V.; Sekaran, S.; Thirumalai, D.; Palaniappan, B. Role of tau protein in Alzheimer's disease: The prime pathological player. *Int. J. Biol. Macromol.* **2020**, *163*, 1599−1617.

(6) Cummings, J.; Zhou, Y.; Lee, G.; Zhong, K.; Fonseca, J.; Cheng, F. Alzheimer's disease drug development pipeline: 2023. *Alzheimers Dement.: Transl. Res. Clin. Interv.* **2023**, *9* (2), No. e12385.

(7) Moussa-Pacha, N. M.; Abdin, S. M.; Omar, H. A.; Alniss, H.; Al-Tel, T. H. BACE1 inhibitors: Current status and future directions in treating Alzheimer's disease. *Med. Res. Rev.* **2020**, *40* (1), 339−384.

(8) Soeda, Y.; Takashima, A. New Insights Into Drug Discovery Targeting Tau Protein. *Front. Mol. Neurosci.* **2020**, *13*, 590896.

(9) Liyanage, S. I.; Weaver, D. F. Chapter Eleven - Misfolded proteins as a therapeutic target in Alzheimer's disease. In *Advances in Protein Chemistry and Structural Biology*; Donev, R., Ed.; Academic Press, 2019; Vol. *118*, pp 371−411.

(10) Zhang, Y.; Chen, H.; Li, R.; Sterling, K.; Song, W. Amyloid β-based therapy for Alzheimer's disease: challenges, successes and future. *Signal Transducti. Target. Ther.* **2023**, *8* (1), 248.

(11) Panza, F.; Lozupone, M.; Logroscino, G.; Imbimbo, B. P. A critical appraisal of amyloid-β-targeting therapies for Alzheimer disease. *Nat. Rev. Neurol.* **2019**, *15* (2), 73−88.

(12) Lee, J. S.; Park, C. B. Microfluidic dissociation and clearance of Alzheimer's β-amyloid aggregates. *Biomaterials* **2010**, *31* (26), 6789−6795.

(13) Knopman, D. S. Lecanemab reduces brain amyloid-β and delays cognitive worsening. *Cell Rep. Med.* **2023**, *4* (3), 100982.

(14) van Dyck, C. H.; Swanson, C. J.; Aisen, P.; Bateman, R. J.; Chen, C.; Gee, M.; Kanekiyo, M.; Li, D.; Reyderman, L.; Cohen, S.; et al. Lecanemab in Early Alzheimer's Disease. *N. Engl. J. Med.* **2023**, *388* (1), 9−21.

(15) Congdon, E. E.; Ji, C.; Tetlow, A. M.; Jiang, Y.; Sigurdsson, E. M. Tau-targeting therapies for Alzheimer disease: current status and future directions. *Nat. Rev. Neurol.* **2023**, *19* (12), 715−736.

(16) Self, W. K.; Holtzman, D. M. Emerging diagnostics and therapeutics for Alzheimer disease. *Nat. Med.* **2023**, *29* (9), 2187−2199.

(17) Stanimirovic, D.; Kemmerich, K.; Haqqani, A. S.; Farrington, G. K. Engineering and pharmacology of blood-brain barrier-permeable bispecific antibodies. *Adv. Pharmacol.* **2014**, *71*, 301−335.

(18) Chen, Z.; Kankala, R. K.; Yang, Z.; Li, W.; Xie, S.; Li, H.; Chen, A. Z.; Zou, L. Antibody-based drug delivery systems for cancer therapy: Mechanisms, challenges, and prospects. *Theranostics* **2022**, *12* (8), 3719−3746.

(19) Biancalana, M.; Koide, S. Molecular mechanism of Thioflavin-T binding to amyloid fibrils. *Biochim. Biophys. Acta* **2010**, *1804* (7), 1405−1412.

(20) Cho, I.; Yoon, S.; Park, S.; Hong, S. W.; Cho, E.; Kim, E.; Kim, H. Y.; Kim, Y. Immobilized Amyloid Hexamer Fragments to Map Active Sites of Amyloid-Targeting Chemicals. *ACS Chem. Neurosci.* **2023**, *14* (1), 9−18.

(21) Wagner, J.; Ryazanov, S.; Leonov, A.; Levin, J.; Shi, S.; Schmidt, F.; Prix, C.; Pan-Montojo, F.; Bertsch, U.; Mitteregger-Kretzschmar, G.; et al. Anle138b: a novel oligomer modulator for disease-modifying therapy of neurodegenerative diseases such as prion and Parkinson's disease. *Acta Neuropathol* **2013**, *125* (6), 795−813.

(22) Shin, J.; Park, S.; Lee, H.; Kim, Y. Thioflavin-positive tau aggregates complicating quantification of amyloid plaques in the brain of 5XFAD transgenic mouse model. *Sci. Rep.* **2021**, *11* (1), 1617.

(23) Kanno, T.; Tsuchiya, A.; Nishizaki, T. Hyperphosphorylation of Tau at Ser396 occurs in the much earlier stage than appearance of learning and memory disorders in 5XFAD mice. *Behav. Brain Res.* **2014**, *274*, 302−306.

(24) Koloteva-Levine, N.; Aubrey, L. D.; Marchante, R.; Purton, T. J.; Hiscock, J. R.; Tuite, M. F.; Xue, W.-F. Amyloid particles facilitate surface-catalyzed cross-seeding by acting as promiscuous nanoparticles. *Proc. Natl. Acad. Sci. U. S. A.* **2021**, *118* (36), No. e2104148118.
(25) Low, K. J. Y.; Venkatraman, A.; Mehta, J. S.; Pervushin, K. Molecular mechanisms of amyloid disaggregation. *J. Adv. Res.* **2022**, *36*, 113−132.
(26) Karikari, T. K.; Nagel, D. A.; Grainger, A.; Clarke-Bland, C.; Crowe, J.; Hill, E. J.; Moffat, K. G. Distinct Conformations, Aggregation and Cellular Internalization of Different Tau Strains. *Front. Cell Neurosci* **2019**, *13*, 296.
(27) Pardridge, W. M. Treatment of Alzheimer's disease and blood-brain barrier drug delivery. *Pharmaceuticals* **2020**, *13* (11), 394.
(28) Matsunaga, Y.; Fujii, A.; Awasthi, A.; Yokotani, J.; Takakura, T.; Yamada, T. Eight-residue Abeta peptides inhibit the aggregation and enzymatic activity of Abeta42. *Regul. Pept.* **2004**, *120* (1−3), 227−236.
(29) Pizzi, A.; Dichiarante, V.; Terraneo, G.; Metrangolo, P. Crystallographic insights into the self-assembly of KLVFF amyloid-beta peptides. *Pept. Sci.* **2018**, *110* (5), e23088.
(30) Tjernberg, L. O.; Näslund, J.; Lindqvist, F.; Johansson, J.; Karlström, A. R.; Thyberg, J.; Terenius, L.; Nordstedt, C. Arrest of beta-amyloid fibril formation by a pentapeptide ligand. *J. Biol. Chem.* **1996**, *271* (15), 8545−8548.
(31) Xiong, N.; Dong, X. Y.; Zheng, J.; Liu, F. F.; Sun, Y. Design of LVFFARK and LVFFARK-functionalized nanoparticles for inhibiting amyloid β-protein fibrillation and cytotoxicity. *ACS Appl. Mater. Interfaces* **2015**, *7* (10), 5650−5662.
(32) Macdonald, J. A.; Bronner, I. F.; Drynan, L.; Fan, J.; Curry, A.; Fraser, G.; Lavenir, I.; Goedert, M. Assembly of transgenic human P301S Tau is necessary for neurodegeneration in murine spinal cord. *Acta Neuropathol. Commun.* **2019**, *7* (1), 44.
(33) Ingham, D. J.; Hillyer, K. M.; McGuire, M. J.; Gamblin, T. C. In vitro Tau Aggregation Inducer Molecules Influence the Effects of MAPT Mutations on Aggregation Dynamics. *Biochemistry* **2022**, *61* (13), 1243−1259.
(34) Bugiani, O.; Murrell, J. R.; Giaccone, G.; Hasegawa, M.; Ghigo, G.; Tabaton, M.; Morbin, M.; Primavera, A.; Carella, F.; Solaro, C.; et al. Frontotemporal dementia and corticobasal degeneration in a family with a P301S mutation in tau. *J. Neuropathol. Exp. Neurol.* **1999**, *58* (6), 667−677.
(35) Oakley, H.; Cole, S. L.; Logan, S.; Maus, E.; Shao, P.; Craft, J.; Guillozet-Bongaarts, A.; Ohno, M.; Disterhoft, J.; Van Eldik, L.; et al. Intraneuronal beta-amyloid aggregates, neurodegeneration, and neuron loss in transgenic mice with five familial Alzheimer's disease mutations: potential factors in amyloid plaque formation. *J. Neurosci.* **2006**, *26* (40), 10129−10140.
(36) Choi, H.-J.; Park, J.-H.; Jeong, Y. J.; Hwang, J.-W.; Lee, S.; Lee, H.; Seol, E.; Kim, I.-w.; Cha, B.-Y.; Seo, J.; et al. Donepezil ameliorates Aβ pathology but not tau pathology in 5xFAD mice. *Mol. Brain* **2022**, *15* (1), 63.
(37) Nelson, P. T.; Braak, H.; Markesbery, W. R. Neuropathology and cognitive impairment in Alzheimer disease: a complex but coherent relationship. *J. Neuropathol. Exp. Neurol.* **2009**, *68* (1), 1−14.
(38) Ganz, A. B.; Beker, N.; Hulsman, M.; Sikkes, S.; Netherlands Brain Bank; Scheltens, P.; Smit, A. B.; Rozemuller, A. J. M.; Hoozemans, J. J. M.; Holstege, H. Neuropathology and cognitive performance in self-reported cognitively healthy centenarians. *Acta Neuropathol. Commun.* **2018**, *6* (64), 61−13.
(39) Nelson, P. T.; Alafuzoff, I.; Bigio, E. H.; Bouras, C.; Braak, H.; Cairns, N. J.; Castellani, R. J.; Crain, B. J.; Davies, P.; Del Tredici, K.; et al. Correlation of Alzheimer disease neuropathologic changes with cognitive status: a review of the literature. *J. Neuropathol. Exp. Neurol.* **2012**, *71* (5), 362−381.
(40) Su, J.; Miao, Q.; Miao, P.; Zhao, Y.; Zhang, Y.; Chen, N.; Zhang, Y.; Ma, S. Pharmacokinetics and Brain Distribution and Metabolite Identification of Coptisine, a Protoberberine Alkaloid with Therapeutic Potential for CNS Disorders, in Rats. *Biol. Pharm. Bull.* **2015**, *38* (10), 1518−1528.
(41) Anand, K. S.; Dhikav, V. Hippocampus in health and disease: An overview. *Ann. Indian Acad. Neurol.* **2012**, *15* (4), 239−246.
(42) Rao, Y. L.; Ganaraja, B.; Murlimanju, B. V.; Joy, T.; Krishnamurthy, A.; Agrawal, A. Hippocampus and its involvement in Alzheimer's disease: a review. *3 Biotech* **2022**, *12* (2), 55.
(43) Volloch, V.; Rits-Volloch, S. Effect of Lecanemab in Early Alzheimer's Disease: Mechanistic Interpretation in the Amyloid Cascade Hypothesis 2.0 Perspective. *J. Alzheimers Dis.* **2023**, *93* (4), 1277−1284.
(44) Cummings, J.; Aisen, P.; Lemere, C.; Atri, A.; Sabbagh, M.; Salloway, S. Aducanumab produced a clinically meaningful benefit in association with amyloid lowering. *Alzheimers Res. Ther.* **2021**, *13* (1), 98.
(45) Boccalini, C.; Ribaldi, F.; Hristovska, I.; Arnone, A.; Peretti, D. E.; Mu, L.; Scheffler, M.; Perani, D.; Frisoni, G. B.; Garibotto, V. The impact of tau deposition and hypometabolism on cognitive impairment and longitudinal cognitive decline. *Alzheimers Dement* **2024**, *20* (1), 221−233.
(46) Yang, N. J.; Hinner, M. J. Getting across the cell membrane: an overview for small molecules, peptides, and proteins. *Methods Mol. Biol.* **2015**, *1266*, 29−53.
(47) Mikitsh, J. L.; Chacko, A. M. Pathways for small molecule delivery to the central nervous system across the blood-brain barrier. *Perspect. Med. Chem.* **2014**, *6*, 11−24.
(48) Xiong, B.; Wang, Y.; Chen, Y.; Xing, S.; Liao, Q.; Chen, Y.; Li, Q.; Li, W.; Sun, H. Strategies for Structural Modification of Small Molecules to Improve Blood−Brain Barrier Penetration: A Recent Perspective. *J. Med. Chem.* **2021**, *64* (18), 13152−13173.
(49) Choi, J. W.; Kim, H. Y.; Jeon, M.; Kim, D. J.; Kim, Y. Efficient access to highly pure β-amyloid peptide by optimized solid-phase synthesis. *Amyloid* **2012**, *19* (3), 133−137.
(50) von Bergen, M.; Barghorn, S.; Biernat, J.; Mandelkow, E.-M.; Mandelkow, E. Tau aggregation is driven by a transition from random coil to beta sheet structure. *Biochim. Biophys. Acta* **2005**, *1739* (2), 158−166.

https://doi.org/10.1021/acsptsci.4c00006
ACS Pharmacol. Transl. Sci. 2024, 7, 2650−2661